

In-flow Self-comminution of Debris-flow and Lahars: Fragmentation and Grinding Experiments for the Dacites from Unzen-Volcano

Christopher GOMEZ^{1,2}, Yoshinori SHINOHARA³, Norifumi HOTTA⁴,
and Haruka TSUNETAKA⁵

¹ Graduate School of Maritime Sciences, SABO Laboratory., Kobe University (Fukae-Minami-Machi, Higashinadaku
5-1-1 Kobe 658-0022, Japan)

E-mail: christophergomez@bear.kobe-u.ac.jp

² Dept. of Geography, University Gadjah Mada (Balaksumur Yogyakarta 55281, Indonesia)

³ Faculty of Agriculture, University of Miyazaki (Gakuen-Kibanadai-nishi 1-1, Miyazaki, 889-2192, Japan)

⁴ Graduate School of Agricultural and Life Sciences, Department of Forestry, University of Tokyo (Yayoi 1-1-1,
Bunkyo-ku, Tokyo, 113-8657, Japan)

⁵ Department of Disaster Prevention, Meteorology and Hydrology, Forest and Forest Products Research Institute (1
Matsunosato, Tsukuba, 305-8687, Japan)

Key Words: debris-flow; lahar; in-flow grinding; grain fragmentation; self-comminution; Unzen Volcano

1. INTRODUCTION

The word lahar originates from the Bahasa Indonesia, where it refers to a slurry of volcanic debris and water flowing on and from volcanic slopes. From this vernacular knowledge, scientists have extended the definition to flows other than Newtonian flows (i.e. stress-strain relationship not being linear), containing at least one debris-flow phase (i.e. the sediment concentration is $> \sim 80\%$ of the mass and $> \sim 60\%$ of volume). They are the equivalent of debris-flows occurring in mountain areas. The slurry often contains a mixture of material ranging from clay-size sediments up to pluri-metric boulders, that are often named over-sized clasts, mixed various types of bio-debris. Direct observation of debris-flows in mountains and lahars on volcanoes are rather scarce¹⁾, due to the nature of the events, their irregular spatio-temporal distribution and the difficulty of access. Scientists have therefore attempted to retrieve flow characteristics from deposits using Ground Penetrating Radar²⁾ or relating deposits to video-observations³⁾, but these recent

investigations have only brought further questions, showing that traditional concepts derived from outcrop analysis for instance had little representativity of lahars or debris-flows⁴⁾.

Consequently, laboratory experiments play a central role in understanding the mechanics and the dynamics of those flows, and in particular it has been shown that the fine-fraction in debris-flows and lahars played a crucial role in the waxing of the flow and thus the runout of an event⁵⁾, while single fraction can play different role being either integrated as part of the slurry or part of the “solid-load”⁶⁾.

The role of the grain-size is further emphasized by their integration in constitutive equations of debris-flows. The formulation by Egashira, Miyamoto and Itoh⁷⁾, writes the dynamic pressure due to inelastic collisions between particles and the shear-stress due to particle inelastic collision as a function of the square of the median grain-size over the vertical velocity gradient (Eq. (1) - (2)).

$$P_d = \rho K_d \frac{\sigma}{\rho} e^2 c^{1/3} d^2 \frac{\partial u}{\partial z} \quad (1)$$

$$\tau_d = \rho K_d (1 - e^2) \left(\frac{\sigma}{\rho}\right) c^{1/3} d^2 \frac{\partial u^2}{\partial z} \quad (2)$$

where, P_d is the collision pressure, τ_d is the shear stress due to particle inelastic collisions, σ is the mass density of particles, ρ is the density of water, K_d is an empirical constant of value 0.0828, u is the velocity.

Furthermore, the grain-size has a well-known effect on the triggering of the debris-flow that can be best modelled by an infinite-plane model, when it does not start off a rotational landslide, with a curved sliding surface, in which case the factor of safety (F_s) can be modelled from the Mohr-Coulomb theory by Eq. 3:

$$\begin{aligned} F_s &= \frac{c + \gamma z \cos^2 \beta \tan \phi}{\gamma z \cos \beta \sin \beta} \\ &= \frac{2c}{\gamma z \sin 2\beta} + \frac{\tan \phi}{\tan \beta} \end{aligned} \quad (3)$$

, which simplifies to eq. 4 when the material is non-cohesive with $c = 0$:

$$F_s = \frac{\tan \phi}{\tan \beta} \quad (4)$$

From these theoretical sets, the present contribution asks whether the ‘ d ’ should be considered as a function of the flow velocity profile, as in-flow comminution (i.e. reduction in size) through fragmentation and grinding may occur, and then reduce the mean and median size of d . Then, in turn, it is expected to impact the triggering of lahars and debris-flows when they occur as a “chain of processes”.

2. OBJECTIVES

The present research is therefore divided into 3 objectives to assess this hypothesis and attempt to provide a preliminary set of measures:

(a) Determine whether in-flow comminution occurs during flowage of debris-flow, and measure it by relating intergranular shock and grinding to grain-size diminution;

(b) Test whether filling the pores of the slurry - ($1 - e$) in eq. 2 – with water influences the comminution process.

(c) For the dacites of Unzen volcano, measure the role of in-flow comminution on the slope stability and the triggering of debris-flows or lahars, using the Mohr-Coulomb’s theory.

3. MATERIAL AND METHODS

(1) Material

Unzen Volcano is located in Nagasaki prefecture (Fig. 1), in Japan, and it has gained unfortunate fame for its last eruption between 1991 and 1995, during which it produced numerous pyroclastic-flows from dome-collapse, from which several lahars/debris-flows occurred.

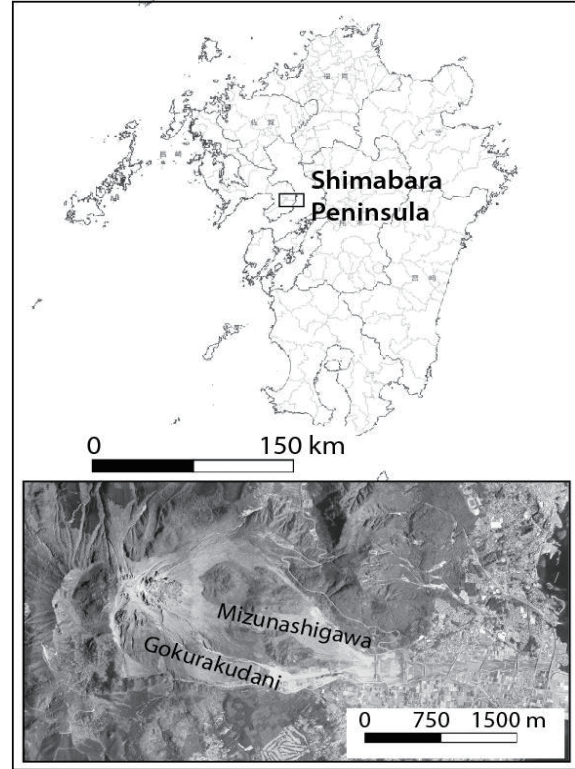


Fig.1 Location of Unzen Volcano in, Kyushu, South-Japan, also showing a zoom on the Mizunashigawa and the Gokurakudani.

The North point upwards on both maps.

A small amount of material collected from a recently formed debris-flow in the Gokurakudani gully, a tributary of the Mizunashigawa - where most of the erupted material was deposited. This set of material was shoveled by hand into container bags and brought back to the laboratory to conduct the present test. No mechanical-engine was used in the collection to avoid altering the material.

(2) Method

The methodological flow has been (1) the collection of dacitic lahar sediment samples at the bottom of the Gokurakudani gully, produced by the 1991-1995 eruption of Unzen Volcano. The material was then separated by dry-sieving between 0.0635 mm and 8 mm, and rolled a set of times in a tumbler adapted from a Los-Angeles abrasion testing machine. In between each set of “material rolling”, the grain size was re-measured. Finally, to assess the role of the generation of fine material by the tumbler on the stability of the deposit, the produced fines

were added to the sieved material to reproduce the data generated by the rotary cylinder.

The impact of fines production was then tested using a direct shear-box. The finest material considered was 0.125 mm, as lower fractions may have more complex impacts and the coarsest material 0.250 mm, as coarser fractions can yield more complex results in the shear-stress box.

(a) Material dry sieving and grains-size

Using a column of sieves composed of 8 stories plus the base (8 mm, 4 mm, 2 mm, 1 mm, 500 μm , 250 μm , 125 μm and 62.5 μm) the material was dried sieved for 2 minutes after collection in the field and **sieving was performed again** after each rolling tumbler experiment. For the material collected in the field and for the experiments involving water in the slurry, the material was dried on a hot plate for 3 hours to a day (depending on the water content), until fully dry. The water was not drained to keep the smallest fractions as well.

(b) Rolling cylinder experiment

The rolling cylinder method uses a Los-Angeles abrasion machine, that has a 0.711 m diameter, as well as a 10 cm shelf built in the cylinder, so that both drop and roll can be performed (video of empty run available here: <https://youtu.be/PHfih1d9D0U>). The rotation angular velocity was set to 45 RPM or 1.6725 $\text{m}\cdot\text{s}^{-1}$ travelled on the perimeter. The speed was controlled with an electric-variator customized to the body of the abrasion machine. Because the simulated fragmentation by block impact is related to the rotation RPM, this signifies that every grain experiences 45 drops per minute (drop height $\frac{1}{2}$ of the cylinder diameter and the mass is the mass of the sediments + 265 g of the container).

Because, we are interested by the inter-granular interactions leading to grinding (supposed by shear-induced friction) and to fragmentation (supposed by collision), the inter-granular space was controlled by placing the dry or wet sediment mixtures into smaller round plastic container to roll and drop within the cylinder. The size of the sediment container is 18 cm in diameter with a capacity of 4 litres. The height h of the sediments was 2 cm at the deepest in the cylinder, ~ 2.4 and ~ 2.9 cm when mixed with 200 g and 400 g of water. The opening of the cylinder was sealed with a double-cap used in the chemical industry. The external cap was then taped to the body to avoid any unscrewing during the experiment. The total energy exerted on the cylinder was measured using an accelerometer placed at the container's end sampling at 10 Hz. At 10 Hz, peak velocity due to the drop were recorded between $|8|$ and $|11|$ $\text{m}\cdot\text{s}^{-1}$ every 8/10 to 9/10 of a second, which is concordant with

the dialed rotation velocity of 45 RPM.

(c) Shear-box testing

The shear-box testing uses a shear box of 30 cm^2 surface, with an electric engine creating a constant shear of 0.8 $\text{mm}\cdot\text{s}^{-1}$ (Tineng Industry AASHTO T236, ASTM D3080). Because the material is $>$ silt and clay, lower shearing speed was not used. Two normal stress were applied to draw the Mohr's circle with two sets of masses 2.5 and 5 kg (plus the mass of the arm) corresponding to 50 kN and 100 kN, or with 100 kN and 200 kN. The horizontal stress was measured using a shearing-ring mounted with a dialed gauge (0.01 mm scale) and the vertical deformation was measured using a 0.01 mm scaled dialed gauge. Because the overlapping surface of the lower-part and the upper-part of the shear box change with the shear, a maximum 5 mm horizontal displacement was used as a maximum.

Using this setup, the fraction $<$ 0.25 mm of samples retrieved from the field was first tested, and then the fraction $<$ 0.25 mm generated from the rotary cylinder was tested. Both dry samples and saturated samples were tested. The dry samples were poured as loose granular material in the shearing box, from a height of 4 cm above the lid (and 6 cm to the bottom of the box) using a funnel. For mixed material, the material was added using a spoon in the funnel to avoid any grading that can occur during pouring the material. For saturated samples, the procedure adopted consisted in filling the lower-box of the shearing box with water, and wait for the already-poured sediment to naturally absorb water by suction. Water was repeatedly added until no more variation was observed over a period of 30 minute for each sample (one will note that the coarse sample took less than a few minutes to stabilize). Finally, between 10 and 20 ml of water was poured over the top porous stone and the water was left to overflow from the lower part of the shear-box for ~ 30 minutes (such process would not be possible with clay and fine-grained sediments). Afterwards, the cap and the bearing were placed over the sample and the sample let to consolidate for ~ 10 minutes, resulting in a vertical variation of 0.1 to 0.25 mm for all the samples. The overflow of water for saturated samples was then cleaned, before the shear test to start.

(d) Sample characteristics

For the present research, four different samples were generated from the material of Unzen volcano, to test in the rotary cylinder experiment (Table 1) and then three different combinations of different grain-sizes were used to test the soil shear strength for both saturated and unsaturated samples leading to 6 samples (Table 2).

During the rotary cylinder experiment, experiment 2 (XP2) failed during the second set of rotations, as the cylinder exploded. For the shear-stress experiment, a technical error occurred during the recording of the unsaturated mix1, and the data were only partial and not included in this contribution (those details are included here as a testimony of the design and the issues in the process).

Table 1 Original samples rotated in the cylinder (T1 is 50% 2-4 mm & 50% > 4 mm; T2: 100% > 4 mm; Rounds: maximum number of rotations applied for each experiment).

XP	Water [g]	Sediments [g]	Size [mm]	Rounds
1	0	400	T1	4484
2	400	400	T1	1484
3	200	400	T1	4484
4	0	400	T2	4484

Table 2 Reconstructed loose samples tested for saturated and unsaturated shear-strength using a shearing box (Sat: saturation and it is divided between unsaturated samples (U) and the saturated ones S). Mix1 corresponds to the grain-size distribution of XP4 for material <0.25 mm and Mix2 XP1 for material < 0.25 mm, which are the two extreme ratios generated by rotating cylinder.

Name	Sat.	Grain size [mm]	σ [kPa]
A1	U	0.25	100 & 200
A2	S	0.25	100 & 200
Mix1	U	80% 0.25, 20% 0.125	100
Mix1	S	80% 0.25, 20% 0.125	100 & 200
Mix2	U	52.5% 0.25, 27.5% 0.125	200 & 400
Mix2	S	52.5% 0.25, 27.5% 0.125	200 & 400

4. RESULTS

(1) Rotary cylinder “self-comminution” results

As a result of the rotations of the cylinder, the original grains reduced in size (Table 3), with the median grain-size being reduced by half for XP 1 and XP 3 and by 30% for XP 2. The reduction was more limited for XP 4.

Although for all experiments the D_{90} does not vary very significantly, the D_{10} changes from 2.1 mm to 1.01 for XP1 and it varies from 4.137 to 0.175 for XP 4. For experiment two and three, D_{10} also reduces, but less significantly.

From Table 3, one can see the rapid reduction of D_{50} for XP1, XP2 and XP3, showing that it is the largest fractions that get broken first, compared to smaller fraction. The rate of this process then decreases. The D_{50} of XP1 reduces by 0.88 every 1,000 rotations, for the first experiment and then by 0.0585 every 1,000 rotations for the 2nd set.

Table 3 D_{10} , D_{50} and D_{90} change through the four experiments (R stands for rotation, with the data before rotation, after 1484 rotations and after 4484 rotations, and XP for experiment).

	D_{10} (mm)	D_{50} (mm)	D_{90} (mm)
XP1 (0 R)	2.139	4.000	5.236
XP1 (1484 R)	2.047	2.692	5.190
XP1 (4484 R)	1.010	2.575	5.130
XP2 (0 R)	2.139	4.000	5.236
XP2 (1484 R)	2.023	2.744	5.216
XP3 (0 R)	2.139	4.000	5.236
XP3 (1484 R)	2.069	2.685	5.184
XP3 (4484 R)	2.014	2.644	5.164
XP4 (0 R)	4.137	4.733	5.415
XP4 (1484 R)	1.049	4.610	5.386
XP4 (4484 R)	0.175	4.504	5.361

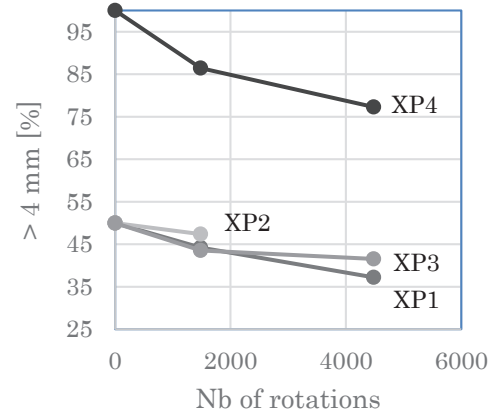


Fig. 2 Comminution of the largest fraction against the number of drums rotations.

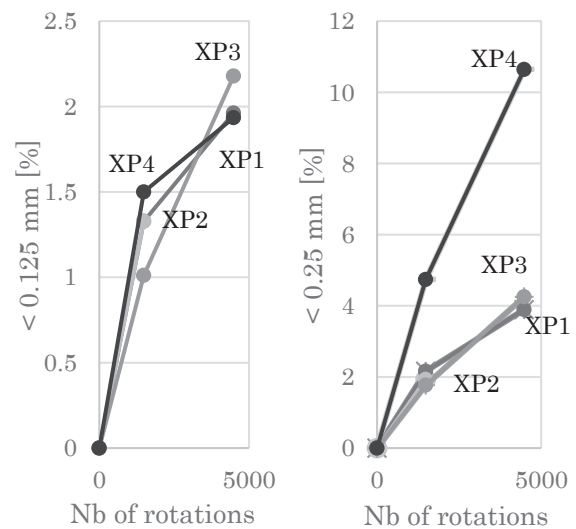


Fig.3 Increase of the fraction inferior to 0.125 mm (a) and 0.25 mm (b).

The same schema appears for XP3. XP2 also shows the same pattern for the first 1484 rotations. However, XP4 shows a more linear decrease, with 0.082 mm per 1,000 rotations, in the first 1484 rotations, and then 0.053 mm per 1,000 rotations in the last 4484 rotations. Although the original fraction still dominates the grain-size distribution, the largest fraction reduces significantly, especially for XP4 (Fig. 2). Furthermore, if the fine sand < 0.125 mm proportion is increasing from none to about 2~2.5 % (Fig. 3-a). The inclusion of the fraction < 0.25 mm shows that XP 4 grinded 12% of sands (Fig. 3-b), so that after 4484 rounds ~ 10% of the mass changed from 0 to 10% of the full mass of the material. All experiments generated < 0.25 mm & > 0.125 fraction, but XP4 has the highest ratio change. For material < 0.125 mm, the ratios are more comparable (Fig. 3-a).

(2) Direct shear-box testing

From the direct shear-box testing, dry unimodal sand of 0.25 mm of diameter displayed the highest shear strength with 177 kPa, while its saturated counterpart reached 173 kPa when a 200 kPa normal stress was applied, displaying little variation. The same characteristics was portrayed with a lower normal stress (100 kPa) as can be seen on fig.4.

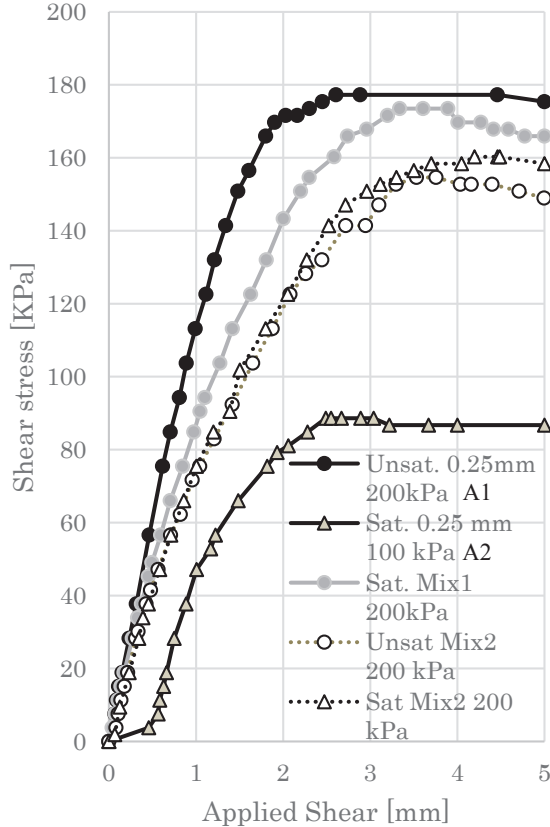


Fig.4 Shear stress pathway change depending on the proportion of fine sands (0.25 mm sand sample are only composed of

0.25 mm sand; “mix1” is 80% of 0.25 mm and 20% of 0.125 mm, and “mix2” is 62.5% of 0.25 mm and 37.5% of 0.125 mm; the values 100 kPa and 200 kPa in the legend represent the normal stress applied).

Applying the Coulomb theory of granular material (Eq. 5), the calculated value of the friction angle in degrees (Φ) varies between 31 degrees and 41 degrees for all the samples, with a positive correlation between the mean grain-size and the friction angle (Fig. 5), i.e. the friction angle increases with mean grain-size.

$$\tau = c + \sigma * \tan \Phi \quad (5)$$

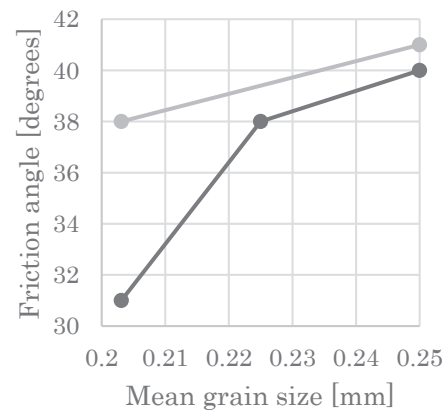


Fig.5 Friction angle calculated from the Mohr-Coulomb theory for loose and dry material (light grey data) and saturated sediments (dark grey data), following the grain-size change.

5. DISCUSSION & CONCLUSION

In-cylinder comminution of the material shows that abrasion and fragmentation occur for both purely granular material and for slurries of materials, which are typical of debris-flows and lahars.

The friction angle data is coherent with published data, that present well-graded sandy gravels between 33 to 40 degrees (or 32 to 44 degrees), and then between 27 to 40 for silts and silty-sands and then between 18 and 32 for silty loam and silty clays⁸.

The present set of experiments from material collected at Unzen Volcano shows that dacites are self-comminuting and that both fragmentation of the larger fractions > 4 mm and > 2 mm is also accompanied by grinding – we suppose by friction and fragmentation of the larger sediment fraction as it would occur in a debris-flow slurry – into material mostly in the range of 125 μ m and smaller. Therefore,

the grain-size distribution of a lahar or a debris-flow deposit is the result of (1) the original material that started the movement, (2) the material eroded from the bed, and (3) the self-comminution processes occurring in the flow. The longer debris-flow runs, the more the 'd' in equations 1 and 2 may need to see a corrector applied.

In turn, it is also expected that this process of material self-comminution is also impacting the triggering of debris-flows and other sediment-laden flows. This was tested for a set of slopes against the factor of safety of the calculated materials and the friction angle reductions (Fig. 6).

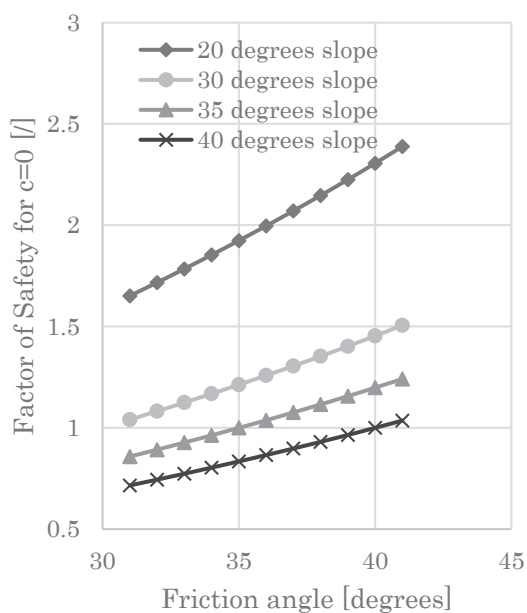


Fig.6 The factor of safety for unconsolidated non-cohesive material as a function of the friction angle for different potential slope angles.

The in-flow self-comminution process should therefore influence the 'd' factor in the constitutive equations but it also should have an impact on the remobilization of the material. It also means that a volume of sediment that starts on a given steep slope can then be remobilized on a slope that is more gentle, because the material itself has changed. This being said, the tail of the lahar and the debris-flow tends to wash away a large portion of the finer fraction when the deposits are not "en masse" and it is therefore difficult to assert the ubiquity of this finding without further investigation. It remains that self-comminution considerations deeply modify the physical underlying of all the equations describing

debris-flows in the literature in Japan and overseas.

Thus, (1) self-comminution occurs in debris flows, and (2) the size of the byproducts change with the proportion of water in the slurry. In the end, (3) this process reduces the shear strength of deposits.

ACKNOWLEDGMENT: The researchers would like to acknowledge the financial assistance provided by the Shimabara Sabo Office, as well as the financial support provided of the Kakenhi-A 18H03957 that have been both instrumental for this research.

REFERENCES

- 1) Imaizumi, F., Tsuchiya, S., Ohsaka, O.: Behaviour of debris flows located in a mountainous torrent on the Ohya landslide, Japan. *Can Geotech J.*, Vol.42, pp.919-931, 2005.
- 2) Starheim, C., Gomez, C., Harrison, J., et al.: Complex internal architecture of a debris-flow deposit revealed using ground-penetrating radar, Cass, New Zealand. *New Zealand Geog.*, Vol. 69, pp. 26-38, 2013.
- 3) Starheim, C., Gomez, C., Davies, T., Lavigne, F., Wassmer, P.: In-flow evolution of lahar deposits from video-imagery with implications for post-event deposit interpretation, Mount Semeru, Indonesia. *J. of Volcanol. Geotherm. Res.*, Vol. 256, pp. 96-104, 2013.
- 4) Gomez, C., Lavigne, F.: Transverse architecture of lahar terraces, inferred from radargrams: preliminary results from Semeru Volcano, Indonesia. *Earth Surf. Proc. Land.*, Vol. 35, 1116-1121, 2010.
- 5) Hotta, N., Kaneko, T., Iwata, T., Nishimoto, H.: Influence of Fine Sediment on the Fluidity of Debris Flows. *J. Mt. Sci.*, Vol.10, pp.233-238, 2013.
- 6) Sakai, Y., Hotta, N., Kaneko, T., Iwata, T.: Effects of Grain-Size Composition on Flow Resistance of Debris Flows: Behavior of Fine Sediment. *H. Hydraul. Eng.*, Vol.145, 06019004-1-7, 2019.
- 7) Egashira, S., Miyamoto, K., Itoh, T.: Constitutive equations of debris flow and their applicability. *Debris-Flow Hazards Mitigation: Mechancis, Prediction and Assessment Proceedings of the First International Conference of Water Resources Engineering Division/ASCE*, pp. 340-349, 1997.
- 8) Geotechdata.info, Angle of Friction, <http://geotechdata.info/parameter/angle-of-friction.html>, 2020

(Received July 1, 2020)